will be published later.
(20) "International Tables for X-Ray Crystallography", Vol. III, Kynoch Press, Birmingham, England, 1968, Section 3.2.
(21) C. T. Prewitt, SFLS5A, SUNY at Stony Brook, modified by M. J. Bennett and B. M. Foxman.
(22) A. Zalkin, FORDAP, Lawrence Berkeley Laboratory, University of California, modified by G. Hamilton and J. A. Ibers.
(23) D. E. Appleman, D. S. Handwerker, and H. T. Evans, Abstracts of the Annual Meeting of the American Crystallographic Association, 1963, pp 42–3.
(24) The conformational energy calculation method is described in detail in H. R. Allcock, R. W. Allen, and J. J. Meister, *Macromolecules*, **9**, 950 (1976). The potential used was a 6–12 Lennard-Jones potential together with a Coulombic term of the type $D_{ij} = (kQ_iQ_j)/(\epsilon r_{ij})$. The partial charges, Q, were +0.70 for phosphorus, −0.32 for nitrogen, and −0.19 for chlorine. No intrinsic backbone torsional potential was applied for the reasons discussed in the article referenced above.
(25) A. J. Hopfinger, "Conformational Properties of Macromolecules", Academic Press, New York, 1973, p 47.
(26) Staff of the Computation Library at Harvard, "The Annals of the Computation Laboratory at Harvard University; Tables of Bessel Functions", Vol. III–VI, Harvard University Press, Cambridge, Mass., 1947.
(27) D. R. Davies and A. Rich, *Acta Crystallogr.*, **12**, 97 (1959).
(28) M. Kakudo and N. Kasai, "X-Ray Diffraction by Polymers", Elsevier, New York, 1972.
(29) C. W. Bunn, "Chemical Crystallography", Oxford University Press, Oxford, 1961.
(30) M. J. Buerger, "X-Ray Crystallography", Wiley, New York, 1942.
(31) One example of the problems encountered is as follows. The meridional rule for a simple 2_1 helix for $(NPCl_2)_n$ ($l = 2n + 1$) can be consequence of a 2_1 screw axis ($00l$, $l = 2n + 1$) or a c glide plane ($0kl$, $l = 2n + 1$, or $h0l$, $l = 2n + 1$). The observed extinctions defined neither a space group nor possible locations of the polymer chain axis.
(32) P. H. Lindenmeyer and R. Hoseman, *J. Appl. Phys.*, **34**, 42 (1963).
(33) G. J. Bullen, *J. Chem. Soc. A*, 1450 (1971).
(34) R. Hazelkamp, T. Migchelson, and A. Vos, *Acta Crystallogr.*, **15**, 539 (1962).
(35) A. J. Wagner and A. Vos, *Acta Crystallogr., Sect. B*, **24**, 707 (1968).
(36) A. W. Schlueter and R. A. Jacobson, *J. Chem. Soc. A*, 2317 (1968).
(37) The equations for these calculations were derived from those reported by T. Miyazawa, *J. Polym. Sci.*, **55**, 215 (1961).
(38) The value of the P–N–P angle depended on the P–N bond distance. For example, for a P–N bond distance of 1.60 Å, the P–N–P angle was 125° (model A, Table V). For a P–N bond distance of 1.52 Å, the P–N–P angle was 141.5° (model E, Table V).
(39) A. Bondi, *J. Phys. Chem.*, **68**, 441 (1964).

Microstructural Characterization of Polypropylenes by High-Resolution Pyrolysis–Hydrogenation Glass Capillary Gas Chromatography

Yoshihiro Sugimura, Tamio Nagaya, and Shin Tsuge*

Department of Synthetic Chemistry, Faculty of Engineering, Nagoya University, Nagoya 464, Japan

Takeshi Murata and Tsunezo Takeda

Analytical Application Laboratory, Shimadzu Seisakusho Ltd., 1-Nishinokyo, Kuwabara-cho, Nakagyo-ku, Kyoto 604, Japan. Received November 6, 1979

ABSTRACT: High-resolution pyrograms of isotactic, syndiotactic, and atactic polypropylenes were obtained by pyrolysis–hydrogenation glass capillary gas chromatography. The assigned characteristic peaks on the pyrograms were interpreted in terms of the stereoregularity and the degree of chemical inversion for the monomer units along the polymer chains.

It is well-known that many physical properties of propylene (PP) are affected not only by the average molecular weight and the molecular weight distribution but also by the stereoregularity and the degree of the chemical inversion in the polymer chain. However, many arguments exist about the polymerization mechanism of olefins, even for Ziegler–Natta catalysts. This is largely responsible for the insufficient and sometimes imprecise information about the microstructures of the resulting polymers. The structural characterization of PP has been carried out most extensively by IR,[1-6] ^{1}H NMR,[7-9] and ^{13}C NMR[10-15] spectral studies. Although the existence of the irregular tail-to-tail linkages of the monomer units along the polymer chain was pointed out by Natta et al.[2] and Tosi et al.,[3] most of the spectroscopic studies were focused on the stereoregularity by asssuming the normal head-to-tail linkages. Recently, Doi et al.[16,17] successfully applied ^{13}C NMR for the elucidation of the chemical inversions in PP.

In addition to the spectroscopic work mentioned above, pyrolysis–gas chromatography (PGC) has been also demonstrated to be a simple, but powerful, technique for studying the microstructures of PP.[18-27] Noffz et al.[20] adopted PGC and used a 100-m-long capillary column to separate the degradation products from various PP's without any hydrogenation. They suggested that qualitative distinction of the PP's differing in the stereoregularity was possible from the resulting diastereomeric olefins. Tsuchiya et al.[22] studied the thermal degradation of PP and pointed out the existence of the irregular monomer placement from resulting 2-methyl-1-hexene.

Most of the other PGC work made use of in-line hydrogenation followed by pyrolysis, using H_2 as a carrier gas in order to convert the resulting degradation products into saturated hydrocarbons.[19,21,24,26] Seeger et al.[26] achieved fairly good separation of the diastereoisomeric products between the trimers and the heptamers and suggested the possibility of estimating the stereoregularity in PP semiquantitatively by comparison with standard PP samples. The resolution of the associated peaks appearing on the reported pyrograms, however, is not still sufficient for complete assignment of the characteristic products.

Recently, we[28,29] developed a method for obtaining high-resolution pyrograms of polymers in which a furnace-type pyrolyzer attached to a high-resolution glass capillary column is used. This technique, employing in-line hydrogenation of the resulting degradation products just before the separation column,[30] was successfully applied to characterization of polyethylenes and ethylene–α-olefin

0024-9297/80/2213-0928$01.00/0 © 1980 American Chemical Society

copolymers. In this work, basically the same technique was utilized for the elucidation of the microstructures in PP. Almost complete separation of the associated peaks between the trimers and the nonamers was achieved. The assigned characteristic peaks on the pyrograms were interpreted in terms of the stereoregularity and the degree of the chemical inversion in PP.

Experimental Section

Samples. Raw material of predominantly isotactic polypropylene (i-PP) was synthesized in the presence of a typical heterogeneous Ziegler-Natta catalyst consisting of a combination of $AlEt_2Cl/TiCl_3$. The i-PP sample was prepared by removing the amorphous portions from the raw material through *n*-hexane extraction. The *n*-hexane soluble fraction in boiling ethyl ether was used as the atactic-polypropylene (a-PP) sample. Syndiotactic polypropylene (s-PP) was synthesized in the presence of a soluble homogeneous catalyst consisting of a combination of $AlEt_2Cl/VCl_4$.

Pyrolysis-Gas Chromatographic Conditions. The pyrolysis-hydrogenation glass capillary gas chromatographic system utilized in this work is basically the same as that described previously.[30] A vertical microfurnace-type pyrolyzer (Yanagimoto GP-1018), described in detail elsewhere,[28,29] was directly attached to a gas chromatograph (Shimadzu 7AG) with a glass capillary column (0.9-mm o.d. × 0.3-mm i.d. × 50-m long) suspension coated by OV-101. A small piece of precut column (3-mm i.d. × 5-cm long) containing 5 wt % of OV-101 packing (80/100 mesh Diasolid-H) and a hydrogenation-catalyst column (3-mm i.d. × 30-cm long) containing 10 wt % of Pt packing (80/100 mesh Diasolid-H) were inserted in series between the pyrolyzer and the splitter. The former precut column was used to protect the catalyst and the separation column from tarry and/or less volatile degradation products. The column temperature was programmed to increase from 40 to 250 °C at a rate of 2 °C/min. A sample of about 200-μg size was pyrolyzed at 650 °C under a flow of hydrogen carrier gas. Most of the peak assignment of the pyrograms was carried out by direct combination of the capillary gas chromatograph with a mass spectrometer (Shimadzu LKB-2091).

Results and Discussion

Stereoregularity. When saturated hydrocarbon polymers such as polyethylene (PE) and PP are exposed to high temperatures under an inert atmosphere, they yield various kinds of hydrocarbon fragments. These degradation products mainly consist of α-olefins, α,ω-diolefins, and alkanes. Therefore, as was reported previously,[29] the pyrograms of PE's consisted of serial triplets. However, as shown in Figure 1, the pyrograms of PP's are not as simple as those of PE's since methyl branchings cause complicated degradation-product patterns. Thus, the resulting α-olefins, α,ω-diolefins, and alkanes are further complicated by the additonal diastereomeric, geometrical, and positional isomers. The number of the possible isomers becomes so large at higher carbon number fragments that the complete chromatographic separation is not a very easy task, even by high-resolution capillary column.

Nevertheless, some conspicuous differences in peak intensity can be observed among the three pyrograms in Figure 1. For example, the doublet peaks of C_{12} (a and b) correspond to monoolefins of *meso*- and *rac*-2,4,6-trimethyl-1-nonenes (**1** and **2**, respectively). i-PP yields a stronger peak for a and s-PP yields a stronger peak for b, while a-PP yields nearly identical peaks for a and b. At larger fragments than pentamers, however, it becomes very difficult to make unequivocal peak assignments.

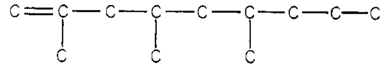

$C{=}\underset{C}{C}-C-\underset{C}{C}-C-\underset{C}{C}-C-C-C$

1

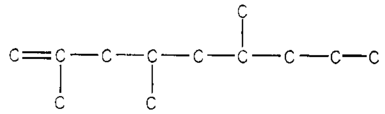

$C{=}\underset{C}{C}-C-\underset{C}{C}-C-\overset{C}{C}-C-C-C$

2

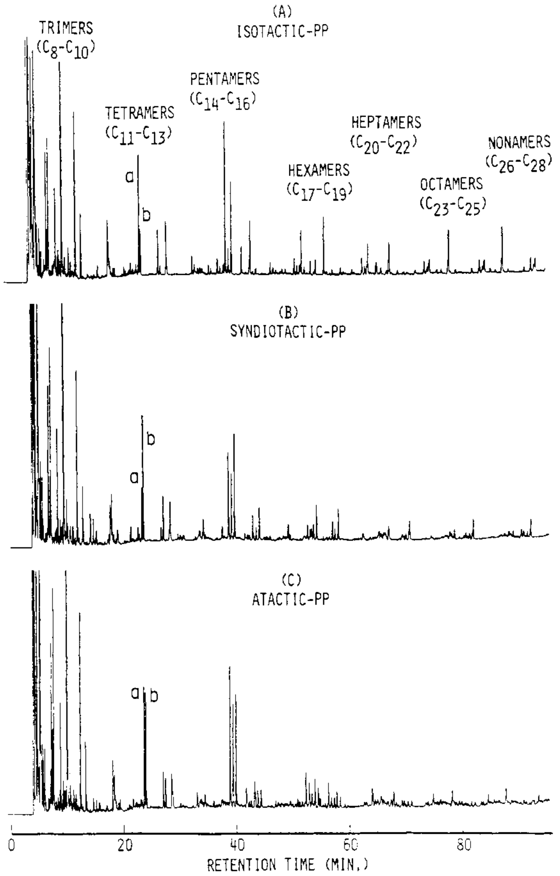

Figure 1. High-resolution pyrograms of (A) i-PP, (B) s-PP, and (C) a-PP without hydrogenation of the degradation products at 650 °C. a and b are peaks for *meso*- and *rac*-2,4,6-trimethyl-1-nonenes, respectively.

On the other hand, as shown in Figure 2, the pyrograms of PP's are characteristically simplified when the degradation products are totally hydrogenated by the hydrogenation catalyst. Thus, otherwise triplet peaks of monoolefin, diolefin, and alkane with the same carbon number are simplified into a singlet, and the final products, mainly consisting of various diastereomeric and positional isomers, are fairly well separated on the pyrograms, even at the heptamers. As was pointed out by Seeger et al.,[26] however, the serial cluster peaks above hexamers become weak in intensity and very complicated because of the large number of possible diastereomeric products.

Therefore, the expanded pyrograms up to pentamer regions are shown in Figure 3 and will be discussed in detail. The main peaks in the trimer region (C_8–C_{10}) are noncharacteristic of the stereoregularity since structures like **3** and **4** are actually the same because of the free rotation of the terminal methyl groups. Accordingly, the tetramers (C_{11}–C_{13}) are the first peaks which reflect the original stereoregularity. Actually, the main tetramer peaks are composed of a triplet of a doublet which corresponds to a meso (m) and racemic (r) pair. For i-PP, the peaks with an m configuration are always stronger than

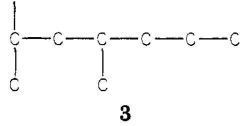

$\overset{C}{\underset{C}{C}}-C-\underset{C}{C}-C-C-C$

3

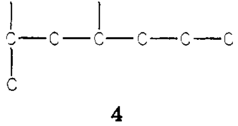

$\overset{C}{\underset{C}{C}}-C-\overset{C}{C}-C-C-C$

4

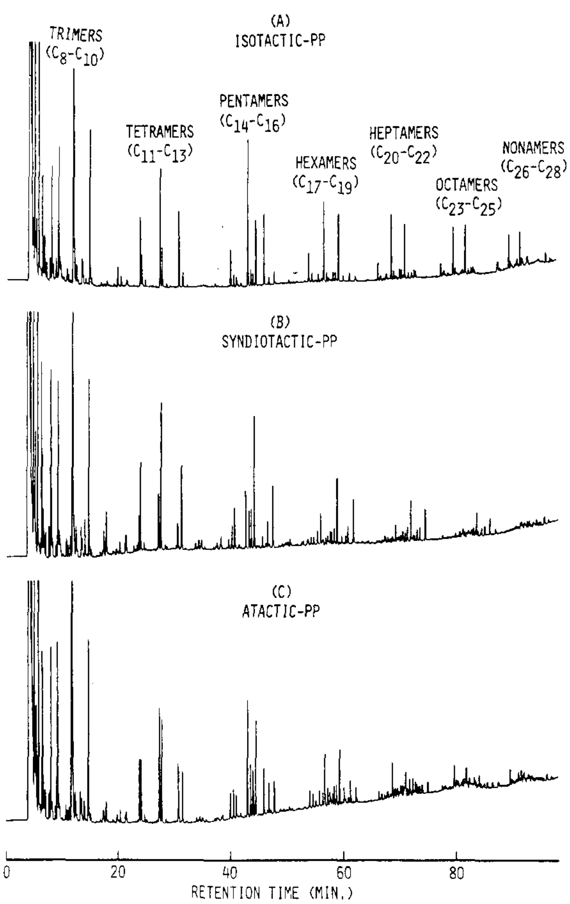

Figure 2. High-resolution pyrograms of (A) i-PP, (B) s-PP, and (C) a-pp after hydrogenation of the degradation products at 650 °C.

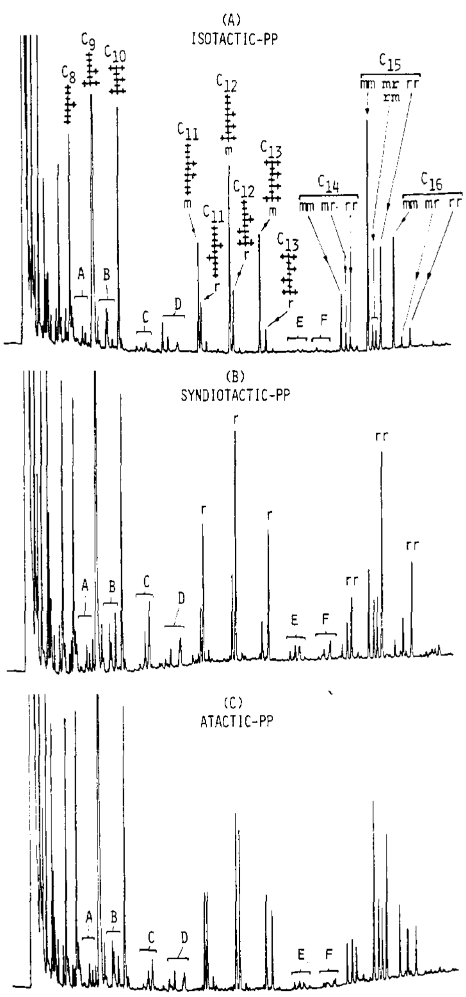

Figure 3. Detailed pyrograms up to heptamer regions for (A) i-PP, (B) s-PP, and (C) a-PP after hydrogenation of the degradation products at 650 °C: C_8–C_{16}, saturated hydrocarbons with 8–16 carbons; m and r, meso and racemic forms, respectively; A–F, minor peaks associated with irregular arrangements of monomer units in the polymer chain.

those with an r configuration. Just the reverse tendency can be observed for s-PP. On the other hand, the peak intensities of the diastereomeric pair are almost equivalent for a-PP.

Similarly, the pentamer clusters of C_{14}, C_{15}, and C_{16} should be composed of a triplet (mm, mr, rr), a quartet (mm, mr, rm, rr) and a triplet (mm, mr, rr), respectively (Chart I). Actually, all the corresponding peaks can be observed on the pyrograms, and mm and rr peaks are characteristic of i-PP and s-PP, respectively, while the peak intensities of mm, mr (plus rm), and rr are nearly identical for a-PP. Thus, qualitative discussion about the stereoregularity in PP's can be made on the basis of the relative intensities among these characteristic diastereomeric isomers of the tetramers and/or the pentamers.

As was pointed out by Seeger et al.,[26] however, the relative peak intensities of these diastereomeric products do not exactly correspond to the original stereoregularities along the polymer chain since isomerization of the diastereomeric products occurs to some extent during pyrolysis at high temperatures.

Here, the reproducibility is fairly good, within 2% of relative standard deviation for the relative intensity measurements of the characteristic peaks. These data suggest that the degree of the isomerization during thermal degradation is almost constant under given pyrolysis conditions. Therefore, this method could be utilized for the practical determination of the stereoregularities if well-characterized samples of PP's are used as reference materials

Chemical Inversions. So far, the stereoregularity in PP's has been discussed only in terms of the main peaks between the trimers and pentamers. However, other minor peaks on the pyrograms of the PP's also provide important information about the microstructures. The peak clusters designated by A–F on the pyrograms in Figure 3 are more or less associated with the irregular positions of the methyl groups along the original polymer chain.

As was discussed in the foregoing section, however, the degradation products above C_{11}, e.g., D–F, should pertain not only to the positional but also to the diastereomeric isomers. Therefore, in the following, the isomers in the trimer region, viz., A (C_8), B (C_9), and C (C_{10}) which mainly reflect differences in the positions of the methyl groups, will be discussed with regard to the irregular attachment of the monomer units.

Before further discussion of the experimental results, we will consider the possible degradation products from the moieties of the irregular attachments along the polymer chain. Here, the methine carbon with methyl branching and the methylene carbon in the monomer unit are defined as the head and tail, respectively:

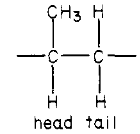

$$-\overset{CH_3}{\underset{H}{C}}-\overset{H}{\underset{H}{C}}-$$

Every C–C bond along the backbone composed of the repeated head-to-tail structures could be regarded as

Chart I

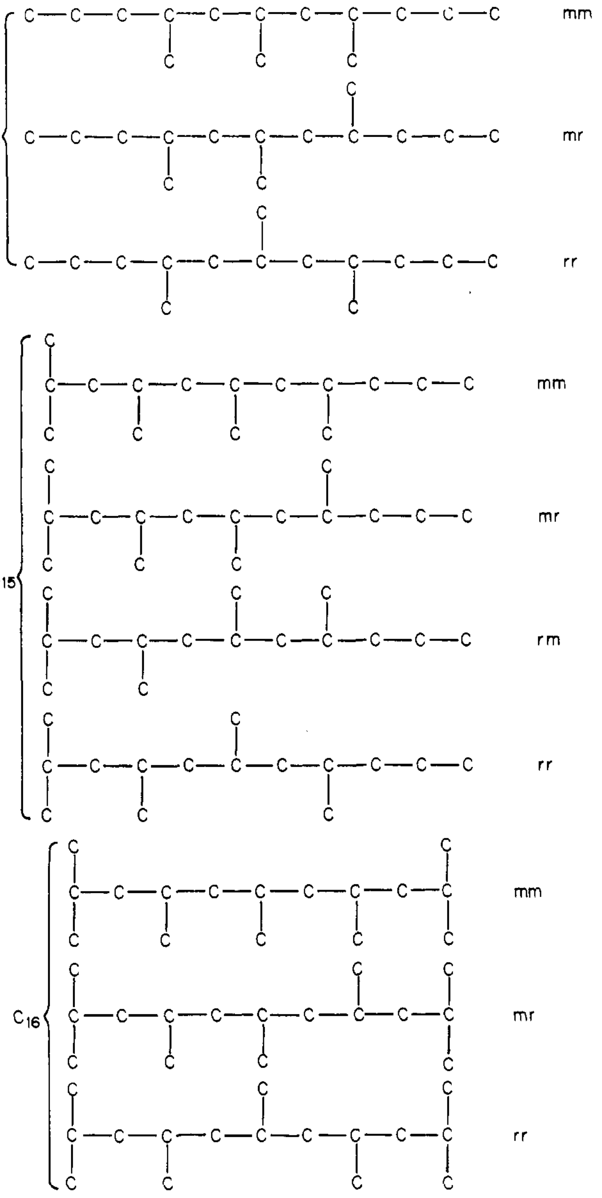

equivalent in bond dissociation energy, provided that differences in the stereoregularities caused negligibly small effects on the bond energy of the backbone. However, when some chemical inversions of the monomer units are supposed to exist, the backbone should have at least three different bondings, as shown in **5**, **6**, and **7**. These cor-

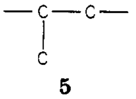

5

$$-\underset{\mathrm{C}}{\mathrm{C}}-\mathrm{C}-$$

$-\mathrm{C}-\mathrm{C}-$

6

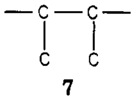

7

$$-\underset{\mathrm{C}}{\mathrm{C}}-\underset{\mathrm{C}}{\mathrm{C}}-$$

respond to the head-to-tail, the tail-to-tail, and the head-to-head linkages, respectively. The bond dissociation energy is in order **6** > **5** > **7**. Therefore, as reported by Tsuchiya et al.,[22] the thermally weakest structure, **7**, is preferentially subject to the thermal cleavage. Actually, the minor degradation products relating to the irregular attachment do not contain any of the **7** structure. Accordingly, in the following discussion, only the **5** and **6** structures are considered for the resulting degradation products associated with the chemical inversions.

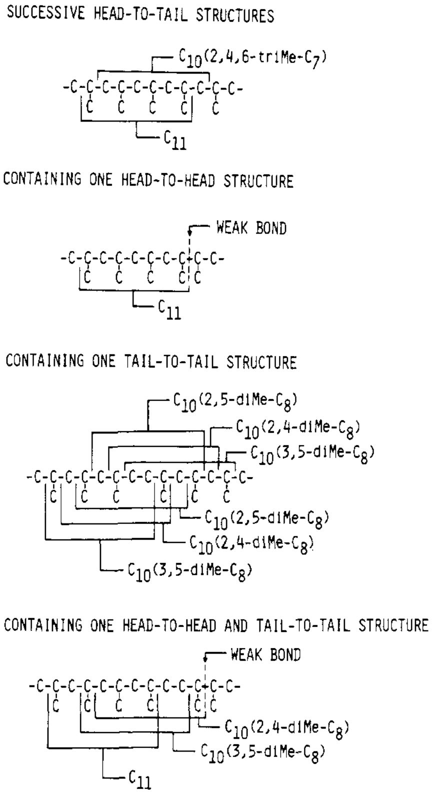

Figure 4. Possible C_{10} products from various structures of PP.

Table I
Peak Assignments of the Trimers

peak[a]	assignment	
a	4-Me-C$_7$	C$_8$
b	side peak 1[b]	
c	2,4-Me$_2$-C$_7$[c]	C$_9$
d	side peak 2[b]	
e	trimethylcyclohexanes	
f		
g	4-Me-C$_8$	
h	2,4,6-Me$_3$-C$_7$	C$_{10}$
i	side peak 3[b]	
j	nonterminal, 2,6-Me$_2$-C$_8$ olefin	
k	2,4-Me$_2$-C$_8$	
l	2,5-Me$_2$-C$_8$, 3,5-Me$_2$-C$_8$	

[a] Peaks correspond to those in Figure 5. [b] Not identified. [c] Main trimer.

Figure 4 illustrates the possible C_{10} products from various moieties of the polymer chain. Here, every degradation product is considered to have been saturated by the hydrogenation catalyst. Thus, the main peak representing the successive head-to-tail structures is 2,4,6-trimethylheptane (Me$_3$-C$_7$). On the other hand, the tail-to-tail structures are reflected by 2,4-, 2,5-, and 3,5-dimethyloctanes (Me$_2$-C$_8$). Similarly, the successive head-to-tail structures for the other possible trimers would yield 4-Me-C$_7$ (C$_8$) and 2,4-Me$_2$-C$_7$ (C$_9$), and the associated chemical inversion peaks would be 2,4- and 2,5-Me$_2$-C$_6$ (C$_8$) and 4-Me-C$_8$ (C$_9$), respectively.

Table I summarizes the assigned peaks around the trimer region of the detailed pyrograms in Figure 5. In addition to the expected products mentioned above, the minor side peaks b (C$_8$), d (C$_9$), i (C$_{10}$), and j (C$_{10}$) can be seen on the pyrograms. Among these, peak j is assigned to nonterminal 2,6-Me$_2$-C$_8$ olefin. This component is most probably formed through demethylation of 2,4,6-Me$_3$-C$_8$ (C$_{11}$) and should be included in the C$_{11}$ main peak. Similarly, nonterminal 2,6-Me$_2$-C$_7$ olefin (C$_9$) formed through demethylation might exist somewhere between the main peaks of C$_9$ (c) and C$_{10}$ (h) and should be included in the C$_{10}$ main peak. However, the contribution of the peak, if

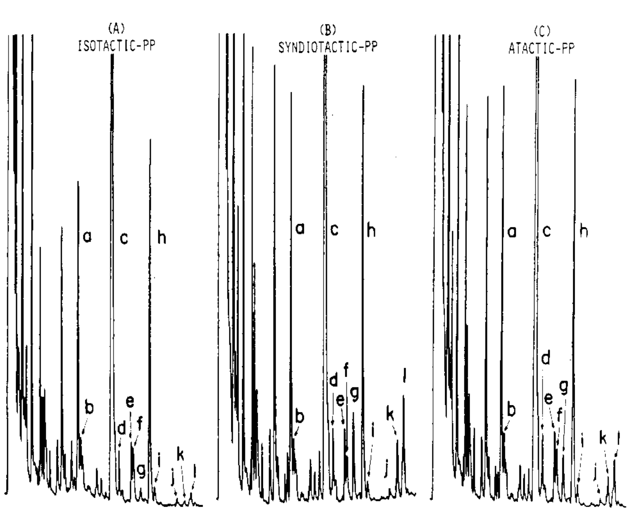

Figure 5. Detailed pyrograms around trimer regions from (A) i-PP, (B) s-PP, and (C) a-PP after hydrogenation of the degradation products at 650 °C. a–l are assigned in Table I.

any, might be negligibly small.

The possible products associated with the tail-to-tail structure for the C_8 cluster are 2,5-Me_2-C_6 and 2,4-Me_2-C_6 which should have appeared before peak a. However, the corresponding peaks were not resolved on the pyrograms.

In the region of C_9, the relative peak intensities of c (2,4-Me_2-C_7, main trimer) and g (4-Me-C_8), which are associated with the tail-to-tail structure, give fairly good information about the chemical inversions along the polymer chain. However, here we should notice fairly strong peaks of trimethylcyclohexanes (e and f) on the pyrograms. The formation of these products can be explained by the possible cyclic intramolecular thermal degradation process. The simple radical transfer of the depropagating macroradical yields the main product of 2,4-Me_2-C_7 as the C_9 trimer. On the other hand, there also exists some probability of forming *cis-* and *trans-*trimethylcyclohexanes since the main chain, consisting of six carbons, just meets the requirement for formation of stable six-membered rings.

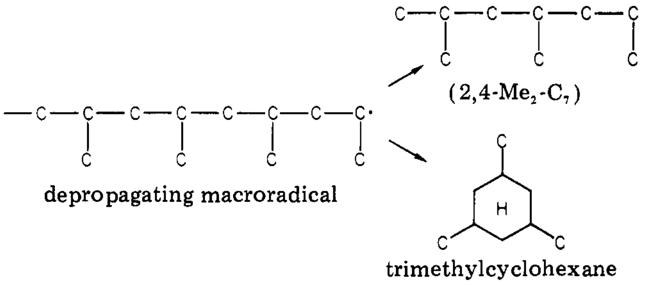

Other possible minor peaks of 1,2,4-trimethylcyclohexane reflecting the irregular structure might be buried in the C_9 cluster. Thus it is very difficult to correlate these peaks quantitatively to the chemical inversions in the polymer chain.

Consequently, the most promising information about the chemical inversions can be obtained from the relative peak intensity between the clearly separated C_{10} peaks of h–l, provided that these products are reflecting the average molecular structures of the original polymer.

Thus, the chemical inversions in PP's were estimated by eq 1, where A is the area of each peak and the factor

$$\%\ \text{tail-to-tail linkage} = \frac{A_k + A_l}{A_h + (A_k + A_l)}\ \frac{1}{3} \times 100 \qquad (1)$$

of $^1/_3$ is needed since one of the three monomer units in the peaks k and l is involved in the tail-to-tail linkage. Here, the side peak of i (C_{10}) was included in the peak h (C_{10}). Thus, the calculated values of the tail-to-tail structure amount to 1.7, 10.8, and 6.3% for i-PP, s-PP, and a-PP, respectively. Only the amounts of the tail-to-tail structure were estimated by this method. However, the polymerization mechanisms of propylene units in the presence of the Ziegler–Natta catalysts predict that almost the same amount of head-to-head structure should be formed in the same chain where the tail-to-tail structure happens to form.[6,31] Therefore, the total amount of chemical inversion might be close to double the tail-to-tail amount.

In our earlier work,[25] total chemical inversions for the same PP's were reported for chlorinated PP samples: 2.6% for i-PP and 9.7% for a-PP. Although the doubled tail-to-tail amounts (3.4% for i-PP and 12.6% for a-PP) are slightly larger than those in the earlier report, they are quite comparable.

The measurements of the relative peak intensities on the pyrograms were repeatable with a standard deviation of less than 5% under the given experimental conditions. Moreover, only 200-μg amounts of the polymer samples were pyrolyzed to get the high-resolution pyrograms and no preliminary sample treatment was made. Therefore, this technique can be used as a rapid and simple method for the routine characterization of PP's.

References and Notes

(1) C. Y. Liang, *J. Polym. Sci.*, **54**, 523 (1961).
(2) G. Natta, A. Valvassori, F. Ciampelli, and G. Mazzanti, *J. Polym. Sci., Part A*, **3**, 1 (1965).
(3) C. Tosi, A. Valvassori, and F. Ciampelli, *Eur. Polym. J.*, **5**, 575 (1969).
(4) Y. Doi, J. Kinoshita, A. Morinaga, and T. Kell, *J. Polym. Sci., Polym. Chem. Ed.*, **13**, 2491 (1975).
(5) J. L. Koenig and A. Van Roggen, *J. Appl. Polym. Sci.*, **9**, 359 (1965).
(6) A. Zambelli, C. Tosi, and C. Sacchi, *Macromolecules*, **5**, 649 (1972).
(7) A. Zambelli, L. Zetta, C. Sacchi, and C. Wolfsgruber, *Macromolecules*, **5**, 440 (1972).
(8) K. Mitani, *J. Macromol. Sci., Chem.*, **A8**, 1033 (1974).
(9) F. C. Stehling and J. R. Knox, *Macromolecules*, **8**, 595 (1975).
(10) L. F. Johnson, F. Heatley, and F. A. Bovey, *Macromolecules*, **3**, 175 (1970).
(11) Y. Inoue, A. Nishioka, and R. Chujo, *Makromol. Chem.*, **152**, 15 (1972); **168**, 163 (1973).
(12) A. Zambelli, D. E. Dorman, A. I. Richard Brewster, and F. A. Bovey, *Macromolecules*, **6**, 925 (1973).
(13) Y. Doi and T. Asakura, *Makromol. Chem.*, **176**, 507 (1975).
(14) J. C. Randall, *J. Polym. Sci., Polym. Phys. Ed.*, **12**, 703 (1974).
(15) A. Zambelli, P. Locatelli, G. Bajo, and F. A. Bovey, *Macromolecules*, **8**, 687 (1975).
(16) T. Asakura, I. Ando, A. Nishioka, Y. Doi, and T. Keii, *Makromol. Chem.*, **178**, 791 (1977).
(17) Y. Doi, *Macromolecules*, **12**, 248 (1979).
(18) B. Groten, *Anal. Chem.*, **36**, 1206 (1964).
(19) J. Van Schooten and J. K. Evenhuis, *Polymer*, **6**, 343 (1965).
(20) D. Noffz, W. Benz, and W. Pfab, *Z. Anal. Chem.*, **235**, 121 (1968).
(21) L. Michajlov, P. Zugenmaier, and H.-J. Cantow, *Polymer*, **9**, 325 (1968).
(22) Y. Tsuchiya and K. Sumi, *J. Polym. Sci., Part A-1*, **7**, 1599 (1969).
(23) Deur-Šiftar and V. Švob, *J. Chromatogr.*, **51**, 59 (1970).
(24) L. Michajlov, H.-J. Cantow, and P. Zugenmaier, *Polymer*, **12**, 70 (1971).
(25) H. Seno, S. Tsuge, and T. Takeuchi, *Makromol. Chem.*, **161**, 185 (1972).
(26) M. Seeger and H.-J. Cantow, *Makromol. Chem.*, **176**, 2059 (1975).
(27) E. Kiran and J. K. Gillham, *J. Appl. Polym. Sci.*, **20**, 2045 (1976).
(28) S. Tsuge and T. Takeuchi, *Anal. Chem.*, **49**, 348 (1977).
(29) Y. Sugimura and S. Tsuge, *Anal. Chem.*, **50**, 1968 (1978).
(30) Y. Sugimura and S. Tsuge, *Macromolecules*, **12**, 512 (1979).
(31) W. L. Carrick, *Adv. Polym. Sci.*, **12**, 65 (1973).